Talanta 280 (2024) 126691

Contents lists available at ScienceDirect

Talanta

journal homepage: www.elsevier.com/locate/talanta

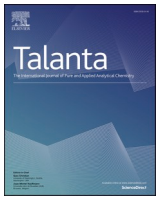

Highly sensitive SERS nanoplatform based on aptamer and vancomycin for detection of *S. aureus* and its clinical application

Shanshan Lin [a,b,d,1], Yunsi Zheng [c,1], Yanlong Xing [a,b], Kun Dou [a,b], Rui Wang [a,b], Hongwang Cui [a,**], Rui Wang [a,b,***], Fabiao Yu [a,b,*]

[a] Key Laboratory of Hainan Trauma and Disaster Rescue, The First Affiliated Hospital of Hainan Medical University, Hainan Medical University, Haikou, 571199, China
[b] Engineering Research Center for Hainan Bio-Smart Materials and Bio-Medical Devices, Key Laboratory of Emergency and Trauma, Ministry of Education, Key Laboratory of Hainan Functional Materials and Molecular Imaging, College of Emergency and Trauma, Hainan Medical University, Haikou, 571199, China
[c] School of Pharmacy, Hainan Medical University, Haikou, 571199, China
[d] Jiangyin Center for Disease Control and Prevention, No. 158 Changjiang Road, Jiangyin, 214431, China

ARTICLE INFO

Handling Editor: A Campiglia

Keywords:
Surface-enhanced Raman scattering (SERS)
S. aureus detection
Dual-recognition
Aptamer and vancomycin

ABSTRACT

Staphylococcus aureus (*S. aureus*) is the most common pathogen in human purulent infections, which can cause local purulent infections, as well as pneumonia, pseudomembranous enteritis, pericarditis, and even systemic infections. The conventional methods including bacteria colony counting, polymerase chain reaction and enzyme-linked immunosorbent assay can't fully meet the requirement of highly sensitive detection of *S. aureus* due to their own disadvantages. Therefore, it's an urgent need to develop new platform to detect *S. aureus* in the early infection stage. In this study, a new surface-enhanced Raman scattering (SERS)-based nanoplatform based on dual-recognition of aptamer (Apt) and vancomycin (Van) was developed for the highly sensitive detection of *S. aureus*. The SERS nanoplatform consisted of two functional parts: aptamer-conjugated Fe_3O_4 magnetic nanoparticles (Fe_3O_4-Apt MNPs) for bacteria enrichment and vancomycin modified-Au nanoparticles (Van-Au NPs) as the SERS probes for *S. aureus* quantitative detection. Upon the target bacteria enrichment, the SERS signals of the supernatant after magnetic separation could be obtained and analyzed under different concentrations of *S. aureus*. The limit of detection of the proposed assay was found to be 3.27 CFU/mL. We believe that the proposed SERS-based nanoplatform has great potential as a powerful tool in the early detection of specific bacteria.

1. Introduction

Staphylococcus aureus (*S. aureus*) is one kind of the most common opportunistic pathogens affecting human survival and is considered to be one of the five leading pathogens associated with infection-related health [1,2]. It can infect almost all tissues, resulting in a variety of diseases including bacteremia, skin and soft tissue infection, ostemyelitis, pneumonia and so on [3,4]. Conventionally, bacterial culture and biochemical identification are considered as the gold standard in the detection of *S. aureus* [5]. However, it needs long culture time even several days due to the pre-enrichment and selective differential plating steps, which limits the rapid detection for clinical diagnosis [6,7]. Polymerase chain reaction (PCR) has been widely used as a powerful tool for bacteria identification; unfortunately, it still needs sample pretreatment procedures including DNA extraction and signal amplification by a sequential thermo-cycling process, which easily induce false-positive signals [8]. Although the enzyme-linked immunosorbent assay (ELISA) holds a variety of advantages including easy use, high stability and

* Corresponding author. Key Laboratory of Hainan Trauma and Disaster Rescue, The First Affiliated Hospital of Hainan Medical University, Hainan Medical University, Haikou, 571199, China.
** Corresponding author. Key Laboratory of Hainan Trauma and Disaster Rescue, The First Affiliated Hospital of Hainan Medical University, Hainan Medical University, Haikou, 571199, China.
*** Corresponding author. Key Laboratory of Hainan Trauma and Disaster Rescue, The First Affiliated Hospital of Hainan Medical University, Hainan Medical University, Haikou, 571199, China.
E-mail addresses: cqchw2013@sina.com (H. Cui), wangrui@hainmc.edu.cn (R. Wang), yufabiao@hainmc.edu.cn (F. Yu).
[1] These authors contributed equally to this work.

https://doi.org/10.1016/j.talanta.2024.126691
Received 11 April 2024; Received in revised form 30 July 2024; Accepted 7 August 2024
Available online 8 August 2024

repeatability, the repeated incubation and washing steps are time-consuming and lacks in sensitivity and specificity [9,10]. Therefore, there is still an urgent need for rapid and specific detection of bacterial pathogens.

Recently, surface-enhanced Raman scattering (SERS) has attracted increasing attention due to its high sensitivity, simple operation and fingerprint spectra, which has been extensively used for the detection of proteins, DNA, bacteria, small molecules and toxic metal ions [11,12]. Two major types of SERS detection, label-free and label-based strategies, have been extensively applied for bacteria identification [13,14]. The former strategy is to directly obtain the Raman spectra of whole-organism fingerprint of bacteria through the close attachment of bacteria cell to SERS active substrates [15]. However, this method is seriously affected by complex matrix and lacks enough sensitivity [16]. In contrast, labeled-based detection is an indirect approach that using SERS probes as quantitative reporters for bacterial detection [17]. More interestingly, the combination of separation tools with SERS probes including magnetic approach, microfluidics and lateral flow assay, can efficiently improve the sensitivity of SERS detection and enrichment of target bacteria in complex samples [18,19]. In addition, one of the key challenges in these methods is to improve the binding efficiency of SERS probes toward the bacteria. Therefore, SERS probes with high sensitivity and specificity are crucial for SERS-based bacterial detection.

Nowadays, SERS probes-bacteria-substrates sandwich immunocomplex is the most common strategy in SERS-based immunoassay with a pair of antibodies or aptamers for recognizing the different antigenic epitopes on the bacteria surface [20,21]. However, the unspecific absorption induced by the cross-linking between antibodies/aptamers and other interferent usually induces the false signals. Thus, the dual-recognition strategy based on different moieties maybe the potential solution to overcome the above obstacle [22–25]. In addition, the volume of immunocomplex is relatively large, making it difficult for the laser spot to fully cover, resulting in significant errors in the detection results. If the volume ratio among SERS probes, bacteria and substrates can be precisely regulated, the quantitative detection of the supernatant separated from the immunocomplex has the great potential to significantly reduce the fluctuations of SERS signals, which will efficiently improve the sensitivity and stability.

Here, we reported a universal SERS-based system with dual-recognition moieties of aptamers and vancomycin (Van) for highly sensitive and specific detection of *S. aureus* by integrating magnetic capture/separation and SERS probes (Van modification) binding. The proposed assay consisted of two steps performed simply in microtubes. The target bacteria were firstly captured and separated from the samples through aptamers conjugated Fe_3O_4 MNPs. Then, SERS probes were introduced to quantify the captured bacteria, which could specifically bind the gram-positive bacteria due to the presence of Van. Finally, the SERS signals for supernatant were recorded through Raman system. With the increasing concentration of *S. aureus*, more bacteria could be captured by Fe_3O_4 MNPs and recognized by SERS probes, resulting in the decreased SERS signals induced by the less SERS probes in the supernatant. The detection limit of *S. aureus* could reach 3.27 CFU/mL, which was much lower than that of the conventional methods. Moreover, the SERS detection method demonstrated high sensitivity for real clinical samples. We believe the proposed method could serve as a powerful detection system for diagnosis of bacterial infection.

2. Experimental section

2.1. Materials

Malachite green isothiocyanate (MGITC) was purchased from Thermo fisher scientific (USA). Gold (III) chloride trihydate ($HAuCl_4{\cdot}3H_2O$) was bought from Siyu Chemcial (Jiangsu, China). Streptavidin magnetic spheres were bought from Beyotime (Shanghai, China). Sulfhydryl-polyethylene glycol-succinimide ester (HS-PEG_{2000}-NHS) was purchased from Ponsure Biotech (Shanghai, China). N-hydroxysulfosuccinimide (NHS) and N-(3-Dimethylaminopropyl)-N′-ethylcarbodiimide hydrochloride (EDC) were bought from Aladdin Biochemical (Shanghai, China). Vancomycin was bought from Macklin Biochemical (Shanghai, China). The streptavidin-Fe_3O_4 MNPs were purchased from Bayotime Biotecnology (Shanghai, China). LB agar medium was bought from Qingdao Hope Bio-Technology (Shandong, China). LB broth medium was purchased from Solarbio Science & Technology (Beijing, China). The S. aureus-Aptamer sequence was synthesized, modified and purified by Sangon Biotech (Shandong, China) with sequence of 5′-Cy5-GCA ATG GTA CGG TAC TTC CTC GGC ACG TTC TCA GTA GCG CTC GCT GGT CAT CCC ACA GCT ACG TCA AAA GTG CAC GCT ACT TTG CTAA- Biotin-3′ [26]. The ultra-pure water (18.25 MΩ cm) used in this study was prepared by a WoTePu water purifier (Sichuan, China) and all the reagents were used directly with no purification. The pipette tips and EP tubes used in the experiment were sterilized by high temperature autoclaving process.

2.2. Instruments

The UV–Vis absorption spectra were measured by MD SpectraMax i3X (Molecular Devices, USA). The Raman measurement were gained by Renishaw inVia Qontor Raman microscope (Renishaw, UK). The laser scanning confocal images were obtained by FV3000 confocal microscope (Olympus, Japan). The dynamic light scattering (DLS) data were collected from the SZ-100Z2 nanoparticle size analyzer (Horiba, Japan). The transmission electron microscope (TEM) images were recorded through the HT7800 instrument (Hitachi, Japan).

2.3. Bacterial culture and plate counting

The experimental strains were purchased from Guangdong Microbial Species Collection Center, including *Staphylococcus aureus* (ATCC 25923), *Escherichia coli* (ATCC 25922), and *Pseudomonas aeruginosa* (ATCC 27853). After bacterial resuscitation, the single colony was inoculated for growth in LB broth medium at a speed of 220 rpm for 10 h. Then the bacteria suspensions were transferred to LB agar plate at dilution of 10^6, 10^7, 10^8. The final concentration of bacteria was determined by counting the colonies and the corresponding OD_{600} values.

2.4. Synthesis of Au NPs

According to the seed growth method, uniform Au NPs with diameter of 40 nm were synthesized [27,28]. The 2.2 mM sodium citrate solution was prepared in a three-necked flask and heated to boiling with strong stirring. Then, 0.5 mL of 25 mM chloroauric acid was immediately added, and kept the boiling for 15 min. It was observed that the solution changed from colorless to light yellow and then changed to light strawberry red. Later the above solution was cooled to 90 °C, 0.5 mL sodium citrate solution (60 mM) and 0.5 mL chloroauric acid solution (25 mM) were added sequentially, with a time interval of 2 min for 12 cycles totally. Afterwards, the temperature was maintained at 90 °C for 30 min, and finally cooled to room temperature.

2.5. Synthesis of gold nanoparticle-vancomycin (Van-Au) SERS probe

1.25 μL, 10^{-4} M of MGITC was added to the above synthesized Au NPs (1 mL), and stirred for 30 min. Vancomycin (Van) solution (4 mg/mL) was prepared, and HS-PEG_{2000}-NHS was mixed with excess vancomycin solution (1:10 of molar mass) at 4 °C overnight in PBS (0.01 M, pH 8.0). Then the post-reaction solution of HS-PEG_{2000}-NHS and vancomycin was added to the Au NPs@MGITC (Au-M NPs), shaking at 4 °C overnight. The centrifugation step (6000 rpm, 10 min) was processed for three times to remove free vancomycin. The final product was resuspended in PBS and stored at 4 °C.

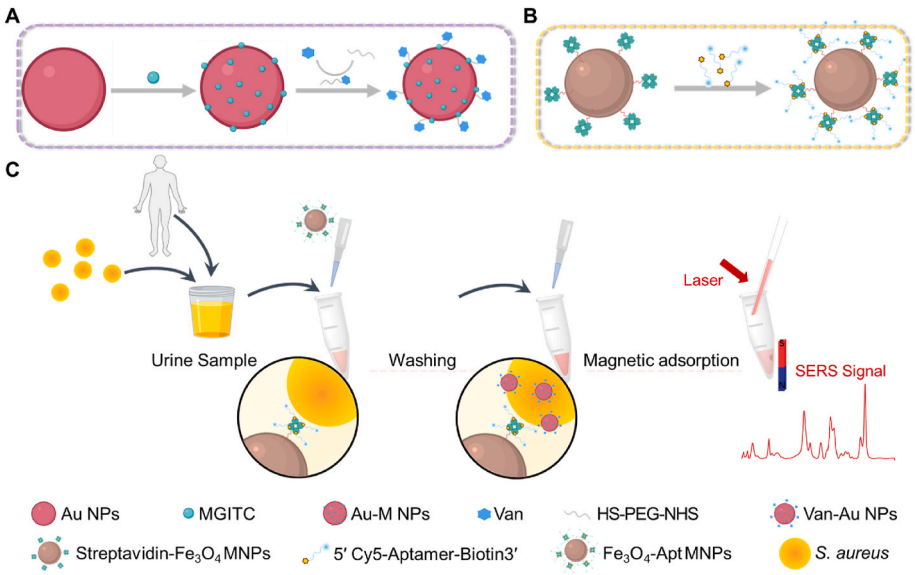

Fig. 1. Schematic illustration of detect *S. aureus* via SERS-based nanoplatform. (A) Preparation of SERS detection probes. (B) Synthesis of magnetic separation platform. (C) The clinical application of SERS-based nanoplatform.

2.6. Synthesis of Fe_3O_4-aptamer capture probes (Fe_3O_4-Apt MNPs)

The aptamer was prepared to 1 μM by adding Tris-EDTA buffer (10 mM Tris-HCl, 1 mM EDTA, pH 8.0) and stored at −20 °C. 40 μL of Fe_3O_4 magnetic nanoparticles were washed twice in 0.5 mL ultra-pure water and resuspended in binding and washing buffer (10 mM Tris-HCl, 1 mM EDTA, 2 M NaCl, pH 7.5). Then 0.6 μL of aptamer solution was added and incubated for 45 min. Next, the excess unbound aptamer was removed and resuspended with binding buffer (0.01 M PBS, 5 mM $MgCl_2$, 1 mM $CaCl_2$, pH 7.4). Finally, the Fe_3O_4-Apt MNPs capture probe was obtained and stored at 4 °C.

2.7. Binding performance of the aptamer to bacteria

10 μL of bacterial suspension (10^7 CFU/mL) was added to 30 μL of aptamer (S. aureus-Aptamer, 100 nM), mixed and shook at 300 rpm for 45 min. Then it was centrifuged twice at 3500 rpm for 5 min and resuspended in PBS. The sample was dropped onto a glass slide to be observed under a confocal fluorescence microscope (E_x: 640 nm, E_m: 650–750 nm).

2.8. Optimization of incubation time between Fe_3O_4-Apt MNPs and bacteria

Fe_3O_4-Apt MNPs were incubated with *S. aureus* for 15, 30, 45, and 60 min, respectively, and the mixture were separated by a magnetic separator. The supernatant and bacterial complex after separation was diluted and transferred to LB plates. The number of colonies formed was counted after 24 h of incubation at 37 °C. The capture rate was calculated as follows:

$$Capture\ Rate = \frac{C_{bacterial\ complex}}{C_{supernatant} + C_{bacterial\ complex}} \times 100\%$$

2.9. Detecting S. aureus with the SERS nanoplatform

10 μL of *S. aureus* bacterial solution with concentrations of 10^7, 10^6, 10^5, 10^4, 10^3, 10^2, 10, and 0 CFU/mL was added to 30 μL Fe_3O_4-Apt MNPs. The mixture was mixed for 45 min, then separated with a magnetic separator and washed to remove non-specifically adsorbed bacteria. 10 μL of SERS probe was added to the above resuspension to fully bind with the *S. aureus* in a constant temperature oscillator at 37 °C. After 20 min of treatment, magnetic separation was applied. The supernatants were sampled by melting point capillary for Raman signal detection. Instrument parameters: 20 × objective, 633 nm laser, 50 % power, exposure time: 1s, cumulative times: 1.

3. Result and discussion

3.1. Principle of SERS-based platform for detection of S. aureus

The aptamer was immobilized on Fe_3O_4 magnetic nanoparticles through biotin-streptavidin system, which was stable and efficient. The bacteria could be captured by the binding between aptamers and specific antigens on the surface of *S. aureus*. Vancomycin could strongly and specially bind the D-Ala-D-Ala moieties in the cell wall of Gram-positive bacteria (such as *S. aureus*), thereby achieving recognition of target bacteria. The vancomycin was modified on the surface of Au NPs as SERS probes through its high affinity for bacterial cell wall precursors. As shown in Fig. 1, the SERS-based nanoplatform for bacterial detection was composed of two components. One component was the Fe_3O_4-Apt MNPs, serving to identify and isolate *S. aureus* in the system, and the other was Van-Au NPs used as SERS probes, which played the recognition role through vancomycin. When the capture probe recognized *S. aureus*, it formed a sandwich structure with the later added recognition probe. The more *S. aureus* were captured, the more SERS probes were enriched, and then the SERS signals in the supernatant were reduced, which could be detected to determine the concentration of bacteria.

3.2. Preparation and characterization of Fe_3O_4-Apt MNPs and SERS probes

Fe_3O_4-Apt MNPs were used for the capture based on the specific aptamer and separation of *S. aureus*. In this work, dual-labeled aptamers with Cy5 and biotin were immobilized on the surface of magnetic beads through the specific binding reaction of biotin and streptavidin as illustrated in Fig. 2A.

The SERS probes were constructed according to the preparation flowchart as shown in Fig. 2B. The MGITC with powerful SERS signals absorbed on the Au NPs to form Au-M NPs. Subsequently, the free amino group in vancomycin and the active ester of NHS formed a stable amide bond through amide condensation reaction [29]. HS-PEG-NHS not only

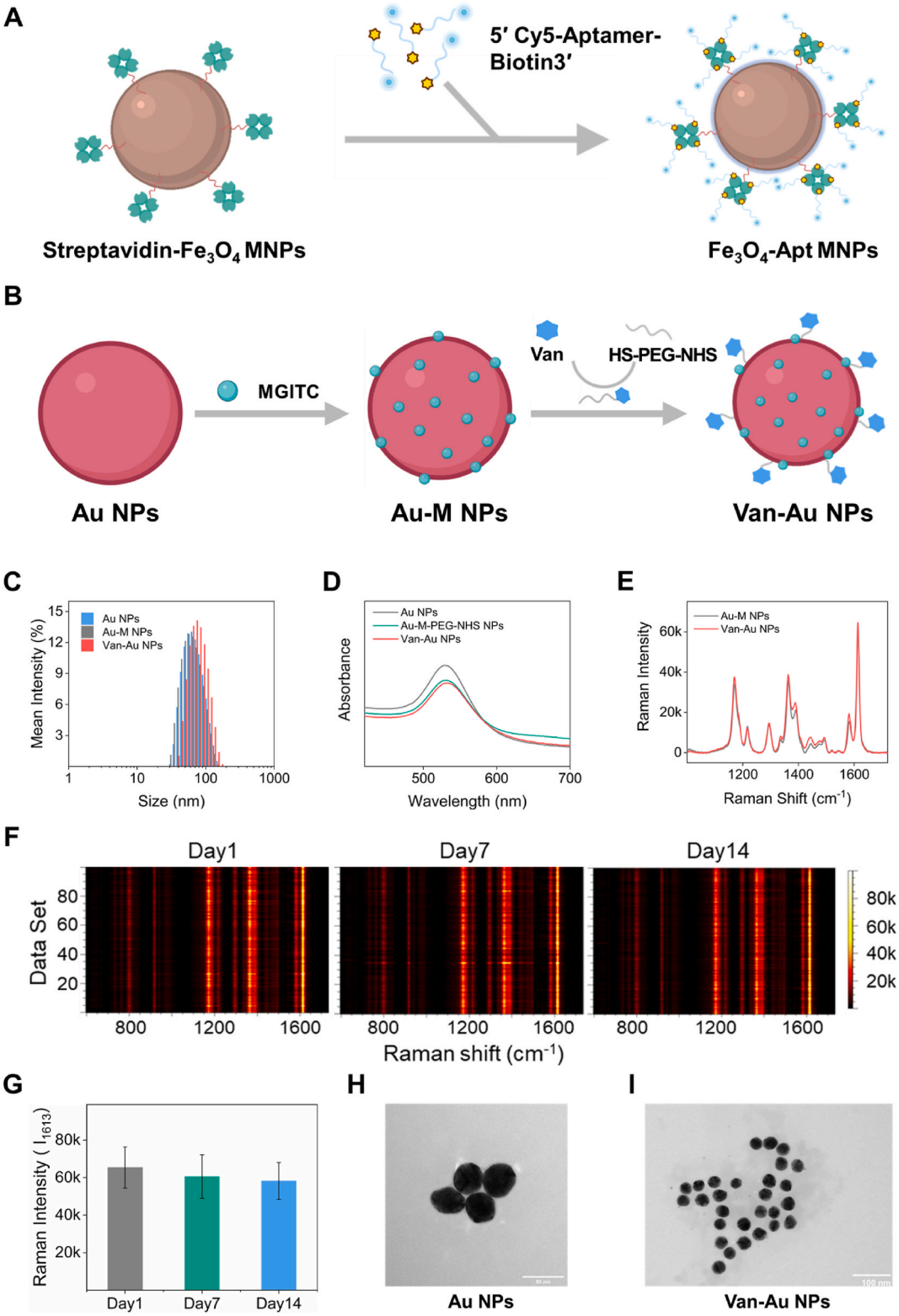

Fig. 2. Preparation and general characterization of Fe_3O_4-Apt MNPs and SERS probes. (A) Schematic diagram of the synthesis of Fe_3O_4-Apt MNPs. (B) Preparation procedure of SERS probes. (C) DLS size of Au NPs, Au-M NPs, and Van-Au NPs. (D) UV–vis absorption spectra of Au NPs, Au-M-PEG-NHS NPs, and Van-Au NPs. (E) Raman spectra of Au-M NPs and Van-Au NPs. (F) The cumulative Raman spectra changes within 14 days. (G) Stability test of SERS probes, the Raman signals was examined on day 1, day 7 and day 14 (n = 100). (H) and (I) TEM image of Au NPs and Van-Au NPs, respectively, scale bar: 50 nm.

provided the protection of the polyethylene glycol layer for the nanoparticles, but also supplied convenience for the attachment of vancomycin [30]. Dynamic light scattering tests showed that the hydrodynamic particle size of Au nanoparticles was 51.5 nm, while the size increased to 55.6 nm after the connection of PEG-Van (Fig. 2C). As depicted in the Zeta potential diagram (Fig. S1), the addition of vancomycin changed the potential towards positive charge, which is consistent with the theoretical basis [31]. The final potential of SERS

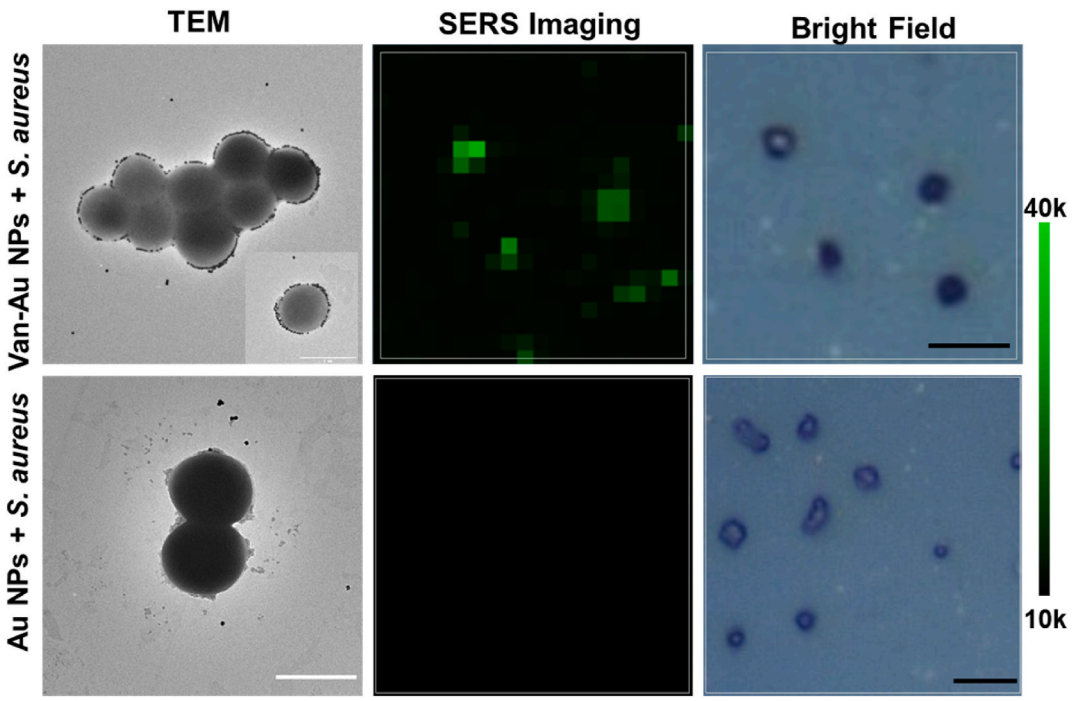

Fig. 3. Recognition of SERS probes to *S. aureus*. TEM images of SERS probes and Au NPs after interaction with *S. aureus*, respectively, scale bar: 1 μm. Representative SERS mapping images at 1613 cm^{-1} of the SERS probe and Au NPs with *S. aureus*, scale bar: 5 μm.

probe was about −49.1 mV, and the absolute value was more than 30, indicating the good stability of Van-Au NPs. As illustrated in Fig. 2D, the changes of maximum absorption peak moved from 529 nm to 533 nm, supporting the successful connection of HS-PEG-NHS and vancomycin. After the modification of vancomycin, the characteristic peak of MGITC remained unchanged and the signal intensity did not significantly decrease (Fig. 2E), which was suggested that the Raman signal could still exist stably after the combination of HS-PEG-Van. In order to further

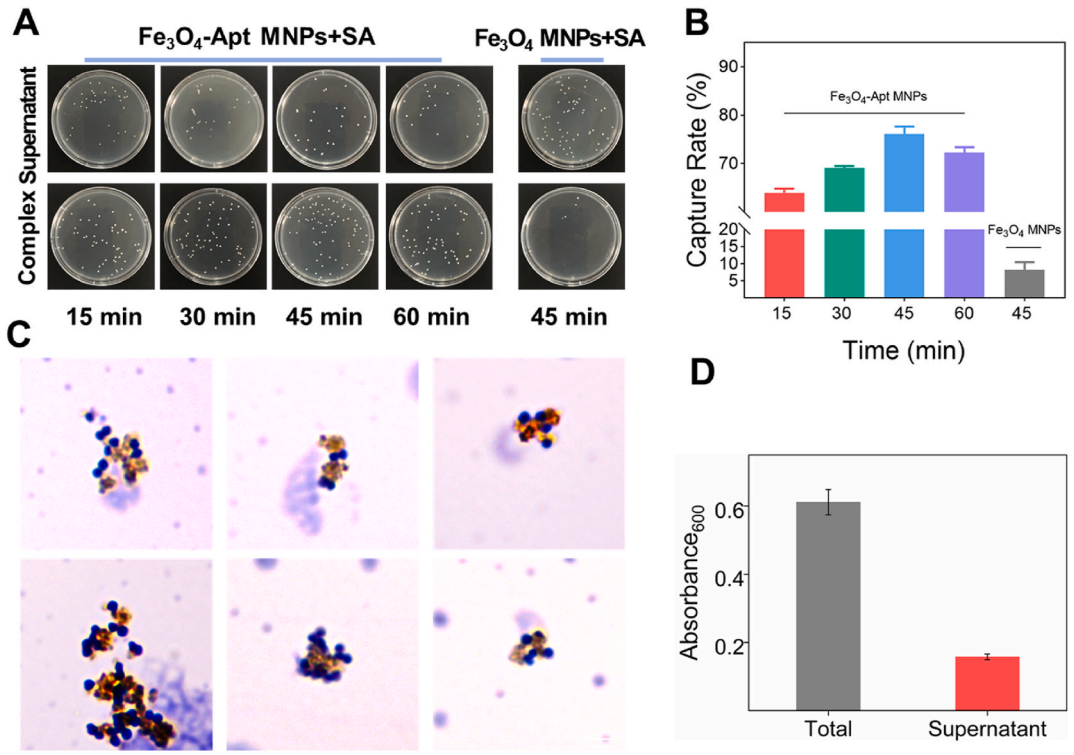

Fig. 4. Capture performance of Fe_3O_4-Apt MNPs for *S. aureus*. (A) Representative bacterial colony formation photographs of Fe_3O_4-Apt MNPs capturing *S. aureus* at 15 min, 30 min, 45 min, and 60 min. Images of bacterial colony formation captured by Fe_3O_4 MNPs at 45 min are shown on the right. (B) Capture rates of *S. aureus* corresponding to (A). (C) Random microscopic images of *S. aureus* captured by Fe_3O_4-Apt MNPs, scale bar: 5 μm. (D) OD_{600} results for total bacterial suspension and supernatant. Experiments were repeated three times and presented as mean ± standard deviation (SD).

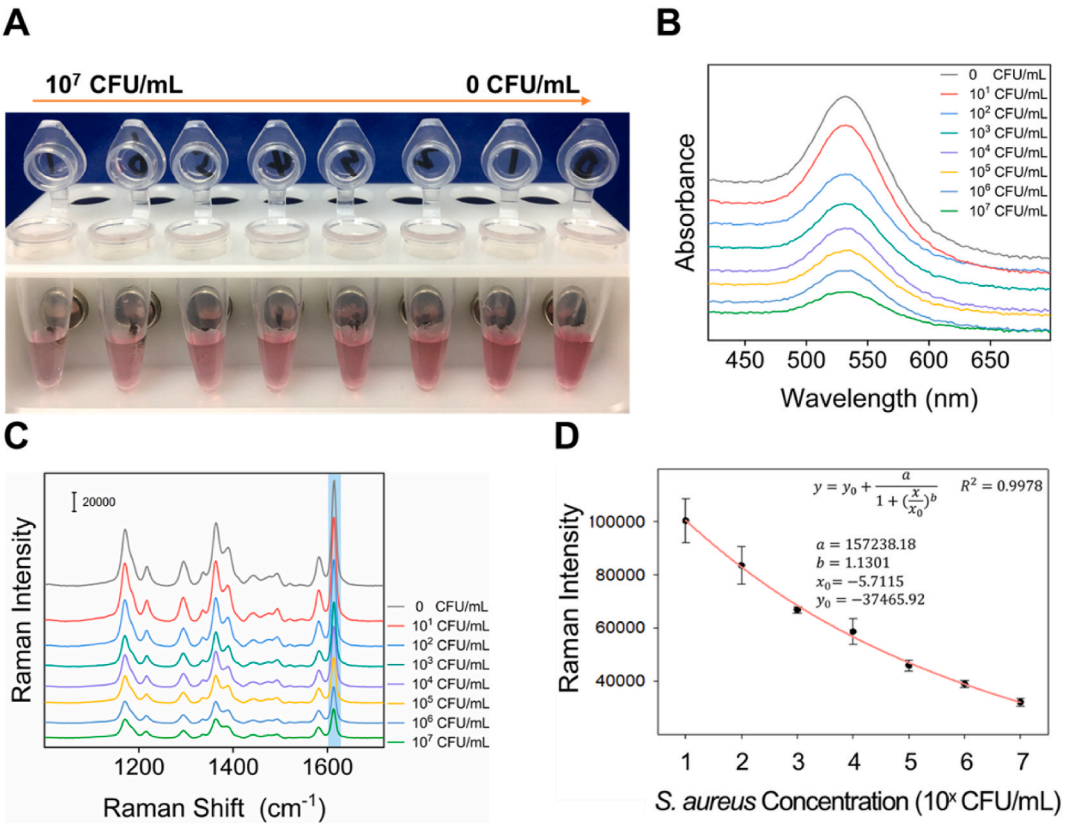

Fig. 5. Detection of *S. aureus* by SERS nanoplatform. (A) The supernatant photograph after incubation. The bacterial concentrations from left to right were 10^7, 10^6, 10^5, 10^4, 10^3, 10^2, 10^1, 0 CFU/mL (B) UV–visible absorption spectra of the supernatant after magnetic separation in A. (C) Raman spectra of the supernatant after magnetic separation in A, with characteristic peak position of 1613 cm^{-1} marked in blue. (D) Fitting curve of Raman signal intensity at 1613 cm^{-1} after treatment with different concentrations of *S. aureus*.

confirm the signal stability, the Raman signals of SERS probes stored at 4 °C were tested on the 1st, 7th and 14th day, respectively. The 100 points were randomly selected each time for signal detection by surface scanning mode. The signal contour map of the 100 signal points each time was shown in Fig. 2F. A plot comparison of Raman signal values at 1613 cm^{-1} showed that the Raman signal decreased by about 11 % from 1st day to 14th day, indicating the reliable stability of SERS probes (Fig. 2G). In addition, Fig. 2H and I exhibited TEM image of Au NPs and SERS probes, from which diameters of the probes were estimated to be 40 nm.

3.3. Recognition of SERS probes to bacteria

To further verify the recognition of SERS probes to *S. aureus*, the SERS probes and Au NPs were fully mixed with *S. aureus* for 20 min, fixed with 2.5 % glutaraldehyde, and observed under the TEM. As indicated in Fig. 3, SERS probes were able to target the *S. aureus*, while only a few Au NPs without vancomycin conjugation were adhered to the bacterial surface. In addition, SERS imaging was used to further examine the targeting performance of the SERS probes with bacteria. The SERS images exhibited the strong SERS signal on the surface of *S. aureus* after incubation with SERS probes. On the contrast, the SERS signals were very low in the Au NPs group. The SERS signal clearly depicted the external outline of the bacteria, indicating excellent recognition ability, which was a crucial step for subsequent detection system.

3.4. Capture efficiency of Fe_3O_4-Apt MNPs to bacteria

The facile construction of the capture substrates was accomplished by immobilizing the S. aureus-aptamer to the surface of Fe_3O_4 magnetic nanoparticles through the ultrahigh binding capability between biotin and streptavidin. Firstly, the targeting performance of the selected aptamer with *S. aureus* was verified. Cy5 was modified at the 5′ end of the aptamer, and the successful match between the aptamer and *S. aureus* was determined by the strong fluorescence signal of Cy5 on the *S. aureus*, as exhibited in Fig. S2. However, there was no obvious fluorescence on the surface of *E. coli*, indicating that the aptamer could specifically bind with *S. aureus*.

As a quite rapid and stable biological reaction system, biotin-avidin binding exhibits high binding affinity and multi-stage amplification effect, which are beneficial to ultrahigh sensitive analysis [32]. The *S. aureus* aptamer with biotin at the 3′ end could be rapidly immobilized to the surface of Fe_3O_4 MNPs modified with streptavidin as shown in Fig. S3, providing favorable conditions for Fe_3O_4-Apt MNPs to efficiently capture *S. aureus*.

To further explore the capture performance of the Fe_3O_4-Apt MNPs for *S. aureus*, a comparison of the capture efficiency at different incubating time was set up. The bacterial colony formation assay was performed, and the colonies were counted to calculate the capture rate (Fig. 4A). The capture rates were 63.9 %, 69.1 %, 76.1 % and 72.2 % with capture time of 15, 30, 45 and 60 min, respectively. Therefore, 45 min was selected as the optimal binding time of Fe_3O_4-Apt MNPs to *S. aureus* as illustrated in Fig. 4B. The randomly selected microscopic images of bacterial complex after gram staining showed that purple *S. aureus* were surrounded by Fe_3O_4-Apt MNPs, which further proved the recognition of Fe_3O_4-Apt MNPs to bacteria. In addition, when Fe_3O_4 MNPs were incubated alone with *S. aureus*, only 8.1 % of the bacteria were present in the bacterial complex. Besides, OD_{600} was used to detect the absorbance of the total bacterial solution and supernatant, and the capture rate was determined to be 74.4 %, in accordance with the results

Table 1
Recovery experiment of *S. aureus* in PBS (n = 3).

Sample NO	Concentration of S. aureu (CFU/mL)	Recovery rate (%)	Standard deviation (%)
1	2×10^6	92.1 %	8.1 %
2	2×10^5	94.6 %	4.2 %
3	2×10^4	92.8 %	6.9 %

of colony forming test.

3.5. SERS detection of S. aureus

Fe_3O_4-Apt MNPs and SERS probes were combined to form an aptamer-based SERS platform for detecting concentrations of *S. aureus* (Fig. 5). Eventually, the supernatant of standard concentrations of *S. aureus* samples (10^7, 10^6, 10^5, 10^4, 10^3, 10^2, 10^1, 0 CFU/mL) was separated by magnetic separator and sampled for SERS signal detection. Fig. 5A exhibited the supernatant photograph after incubation, which demonstrated that with the increase of bacterial concentration, the pink color of the SERS probes in the supernatant gradually faded. The UV–vis results also supported the above phenomenon (Fig. 5B). The Raman intensity of MGITC at 1613 cm^{-1} was monitored to quantify *S. aureus* concentration as shown in Fig. 5C. The concentration of *S. aureus* varied from 0 to 10^7 CFU/mL. Conversely, as the concentration of *S. aureus* increased, more *S. aureus* could be formed bacterial complex with Fe_3O_4-Apt MNPs, resulting in more SERS probes were attached to the surface of magnetic beads. Thus, the Raman signal intensity of the supernatant was correspondingly decreased with increasing *S. aureus* concentration. On the basis of the Raman intensity at 1613 cm^{-1}, the fitting curve for the quantitative analysis of *S. aureus* was constructed, which was determined from the sigmoid function in Fig. 5D. The error bars indicated the standard deviation of three measurements. The limit of detection (LOD) for the SERS based method, estimated as three standard deviations from the background, was 3.27 CFU/mL.

Subsequently, the selectivity of SERS nanoplatform for *S. aureus* was analyzed with the other interfering bacteria. Blank, *E. coli* (10^7 CFU/mL), *P. aeruginosa* (10^7 CFU/mL), *S. pyogenes* (10^7 CFU/mL), *B. subtilis* (10^7 CFU/mL), *S. aureus* (10^5 CFU/mL) and mixed bacterial samples (suspension of three bacteria) were used as samples for SERS detection. The results in Fig. S4 showed that Fe_3O_4-Apt MNPs could hardly capture high concentration of *E. coli* and *P. aeruginosa*, and the final SERS signal intensity was similar to that of the blank group. However, in the low concentration sample of *S. aureus,* the intensity of SERS signal significantly reduced, due to the capture of *S. aureus* by Fe_3O_4-Apt MNPs. Simultaneously, the presence of *S. aureus* could also be detected in mixed samples, indicating that this nanoplatform was specific for the detection of *S. aureus*, which also meant that the detection strategy could be used for mixed bacterial samples.

3.6. Recovery test

S. aureus samples (2×10^6, 2×10^5, 2×10^4 CFU/mL) were prepared with PBS, and SERS signals were measured under the above conditions. The recovery rates of PBS samples were 92.1 %, 94.6 % and 92.8 %, respectively (Table 1 and Fig. 6A), which proved the feasibility of the SERS nanoplatform to detect bacterial samples. In order to evaluate the feasibility of the SERS platform in body fluid, the recovery rate of urine samples was tested. Fresh urine was filtered in 0.22 μm, and *S. aureus* was added to achieve the final concentration of 2×10^6, 2×10^5, and 2×10^4 CFU/mL. The recovery rates were 99.4 %, 97.6 %, and 92.4 %, respectively, as shown in Table 2 and Fig. 6B, which demonstrated the

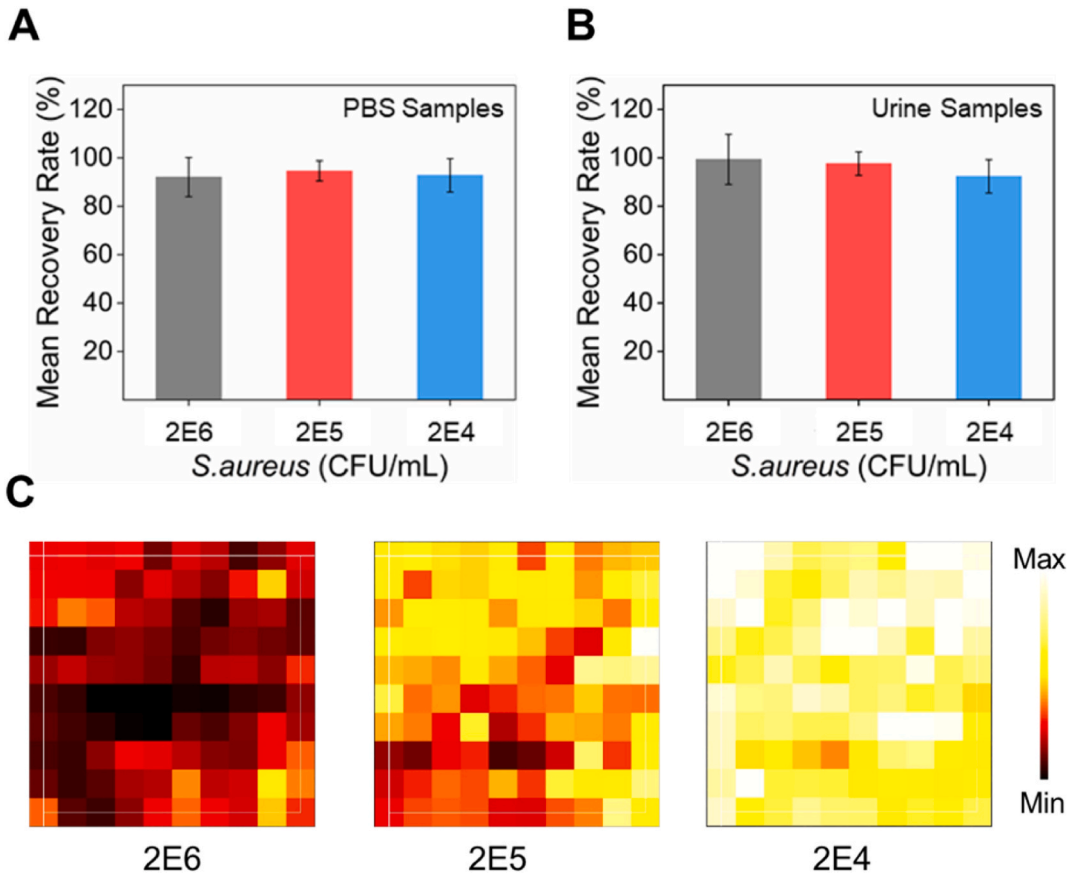

Fig. 6. Spiked recovery test of *S. aureus* by SERS nanoplatform (A) Spiked recovery data of *S. aureus* in PBS. (B) Spiked recovery of *S. aureus* in urine. (C) SERS Mapping of I_{1613} for *S. aureus* detection in urine, scale bar: 5 μm, n = 100.

Table 2
Recovery experiment of *S. aureus* in urine sample (n = 3).

Sample NO	Concentration of S. aureu (CFU/mL)	Recovery rate (%)	Standard deviation (%)
1	2×10^6	99.4 %	10.3 %
2	2×10^5	97.6 %	4.9 %
3	2×10^4	92.4 %	6.9 %

accuracy of using this SERS detection method for bacterial detection under urine milieu. To further check the accuracy of recovery tests, SERS mapping was used for imaging analysis of bacteria samples in urine. The step path was 3 μm, and 10 × 10 points were taken for SERS imaging. It was displayed that with the increasing bacterial concentration, the SERS signal intensity gradually decreased, which proved the trend between the SERS detection results and the concentration.

4. Conclusion

In summary, we developed a highly sensitive and dual-recognition SERS platform for detection of *S. aureus*. The formed SERS probes exhibited uniform size and stable SERS signal. The Fe_3O_4-Apt MNPs using as the substrate could achieve excellent capture efficiency on *S. aureus*. The SERS signal of the supernatant showed a negative relationship between the bacterial concentration and SERS signal intensity with the limit of detection of 3.27 CFU/mL. Urine bacterial samples could also be detected and quantified in this platform with satisfactory recovery. This SERS nanoplatform based on aptamers has the advantages of simple processing, low dosage and high detection sensitivity, which is expected to be a promising method for rapid and sensitive detection of bacteria.

CRediT authorship contribution statement

Shanshan Lin: Writing – original draft, Formal analysis, Data curation, Conceptualization. **Yunsi Zheng:** Writing – original draft, Methodology, Investigation, Conceptualization. **Yanlong Xing:** Software, Resources, Formal analysis. **Kun Dou:** Writing – review & editing, Methodology, Investigation, Formal analysis. **Rui Wang:** Writing – review & editing, Validation, Resources. **Hongwang Cui:** Methodology, Investigation, Data curation. **Rui Wang:** Writing – review & editing, Validation, Supervision, Funding acquisition, Conceptualization. **Fabiao Yu:** Writing – review & editing, Validation, Methodology, Funding acquisition.

Declaration of competing interest

The authors declare that they have no known competing financial interests or personal relationships that could have appeared to influence the work reported in this paper.

Data availability

Data will be made available on request.

Acknowledgements

This work was supported by the Hainan Province Science and Technology Special Fund (ZDYF2024SHFZ104), National Natural Science Foundation of China (Grant No. 22264013, and 22204037), Natural Science Research Talent Project of Hainan Medical University (Grant No. JBGS202101), Hainan Province Science and Technology Special Fund (ZDYF2022SHFZ288), Hainan Provincial Natural Science Foundation of China (Grant No. 820RC654 and 823MS050), Hainan Province Clinical Medical Center (2021), Nanhai Young-Talent Program of Hainan (Grant No. 20202007), Project for Functional Materials and Molecular Imaging Science Innovation Group of Hainan Medical University.

Appendix A. Supplementary data

Supplementary data to this article can be found online at https://doi.org/10.1016/j.talanta.2024.126691.

References

[1] B.P. Howden, S.G. Giulieri, T. Wong Fok Lung, S.L. Baines, L.K. Sharkey, J.Y. Lee, A. Hachani, I.R. Monk, T.P. Stinear, Staphylococcus aureus host interactions and adaptation, Nat. Rev. Microbiol. 21 (2023) 380–395.
[2] N.A. Turner, B.K. Sharma-Kuinkel, S.A. Maskarinec, E.M. Eichenberger, P.P. Shah, M. Carugati, T.L. Holland, V.G. Fowler, Methicillin-resistant Staphylococcus aureus: an overview of basic and clinical research, Nat. Rev. Microbiol. 17 (2019) 203–218.
[3] J.M. Kwiecinski, A.R. Horswill, Staphylococcus aureus bloodstream infections: pathogenesis and regulatory mechanisms, Curr. Opin. Microbiol. 53 (2020) 51–60.
[4] T.J. Foster, A. J Geoghegan, V.K. Ganesh, M. Höök, Adhesion, invasion and evasion: the many functions of the surface proteins of Staphylococcus aureus, Nat. Rev. Microbiol. 12 (2014) 49–62.
[5] H. Sohrabi, M.R. Majidi, P. Khaki, A. Jahanban-Esfahlan, M. de la Guardia, A. Mokhtarzadeh, State of the art: lateral flow assays toward the point-of-care foodborne pathogenic bacteria detection in food samples, Compr. Rev. Food Sci. Food Saf. 211 (2022) 868–1912.
[6] L. Váradi, J.L. Luo, D.E. Hibbs, J.D. Perry, R.J. Anderson, S. Orenga, P. W. Groundwater, Methods for the detection and identification of pathogenic bacteria: past, present, and future, Chem. Soc. Rev. 46 (2017) 4818–4832.
[7] P. Rajapaksha, A. Elbourne, S. Gangadoo, R. Brown, D. Cozzolino, J. Chapman, A review of methods for the detection of pathogenic microorganisms, Analyst 144 (2019) 396–411.
[8] S. Huber, J. Weinberger, M. Pilecky, I. Lorenz, A. Schildberger, V. Weber, S. Fuchs, W. Posch, L. Knabl, R. Würzner, A.E. Posch, D. Orth-Höller, A high leukocyte count and administration of hydrocortisone hamper PCR-based diagnostics for bloodstream infections, Eur. J. Clin. Microbiol. Infect. Dis. 40 (2021) 1441–1449.
[9] A. Nouri, H. Ahari, D. Shahbazzadeh, Designing a direct ELISA kit for the detection of Staphylococcus aureus enterotoxin A in raw milk samples, Int. J. Biol. Macromol. 107 (2018) 1732–1737.
[10] X. Qi, Y. Ye, H. Wang, B. Zhao, L. Xu, Y. Zhang, X. Wang, N. Zhou, An ultrasensitive and dual-recognition SERS biosensor based on Fe_3O_4@Au-Teicoplanin and aptamer functionalized Au@Ag nanoparticles for detection of Staphylococcus aureus, Talanta 250 (2022) 123648.
[11] T. Itoh, M. Procházka, Z.C. Dong, W. Ji, Y.S. Yamamoto, Y. Zhang, Y. Ozaki, Toward a new era of SERS and TERS at the nanometer scale: from fundamentals to innovative applications, Chem. Rev. 123 (2023) 1552–1634.
[12] T. Gong, C.M. Das, M.-J. Yin, T.-R. Lv, N.M. Singh, A.M. Soehartono, G. Singh, Q.-F. An, K.-T. Yong, Development of SERS tags for human diseases screening and detection, Coord. Chem. Rev. 470 (2022) 214711.
[13] A. Zhu, S. Ali, T. Jiao, Z. Wang, Q. Ouyang, Q. Chen, Advances in surface-enhanced Raman spectroscopy technology for detection of foodborne pathogens, Compr. Rev. Food Sci. Food Saf. 22 (2023) 1466–1494.
[14] X. Zhou, Z. Hu, D. Yang, S. Xie, Z. Jiang, R. Niessner, C. Haisch, H. Zhou, P. Sun, Bacteria detection: from powerful SERS to its advanced compatible techniques, Adv. Sci. 7 (2020) 2001739.
[15] D.D. Galvan, Q. Yu, Surface-enhanced Raman scattering for rapid detection and characterization of antibiotic-resistant bacteria, Adv. Healthcare Mater. 7 (2018) e1701335.
[16] M. Usman, J.W. Tang, F. Li, J.X. Lai, Q.H. Liu, W. Liu, L. Wang, Recent advances in surface enhanced Raman spectroscopy for bacterial pathogen identifications, J. Adv. Res. 22 (2022), 00266-1.
[17] H. Liu, X. Gao, C. Xu, D. Liu, SERS tags for biomedical detection and bioimaging, Theranostics 12 (2022) 1870–1903.
[18] R. Wang, K. Kim, N. Choi, X. Wang, J. Lee, J.H. Jeon, G. Rhie, J. Choo, Highly sensitive detection of high-risk bacterial pathogens using SERS-based lateral flow assay strips, Sens. Actuators B Chem. 270 (2018) 72–79.
[19] L. Jiang, M.M. Hassan, S. Ali, H. Li, R. Sheng, Q. Chen, Evolving trends in SERS-based techniques for food quality and safety: a review, Trends Food Sci. Technol. 112 (2021) 225–240.
[20] G. Jiang, Y. Li, J. Liu, L. Liu, F. Pi, Progress on aptamer-based SERS sensors for food safety and quality assessment: methodology, current applications and future trends, Crit. Rev. Food Sci. Nutr. 64 (2024) 783–800.
[21] H. Shen, J. Wang, H. Liu, Z. Li, F. Jiang, F.-B. Wang, Q. Yuan, Rapid and selective detection of pathogenic bacteria in bloodstream infections with aptamer-based recognition, ACS Appl. Mater. Interfaces 8 (2016) 19371–19378.
[22] Z. Zhou, R. Xiao, S. Cheng, S. Wang, L. Shi, C. Wang, K. Qi, S. Wang, A universal SERS-label immunoassay for pathogen bacteria detection based on Fe_3O_4@Au-aptamer separation and antibody-protein A orientation recognition, Anal. Chim. Acta 1160 (2021) 338421.
[23] A. Zhu, S. Ali, Y. Xu, Q. Ouyang, Q. Chen, A SERS aptasensor based on AuNPs functionalized PDMS film for selective and sensitive detection of Staphylococcus aureus, Biosens. Bioelectron. 172 (2021) 112806.

[24] F. Liu, J. Zhao, X. Liu, X. Zhen, Q. Feng, Y. Gu, G. Yang, L. Qu, J.J. Zhu, PEC-SERS dual-mode detection of foodborne pathogens based on binding-induced DNA walker and C_3N_4/MXene-Au NPs accelerator, Anal. Chem. 95 (2023) 14297–14307.
[25] J. Wang, H. Jiang, Y. Chen, X. Zhu, Q. Wu, W. Chen, Q. Zhao, J. Wang, P. Qin, CRISPR/Cas9-mediated SERS/colorimetric dual-mode lateral flow platform combined with smartphone for rapid and sensitive detection of Staphylococcus aureus, Biosens. Bioelectron. 249 (2024) 116046.
[26] Y. Lian, F. He, H. Wang, F. Tong, A new aptamer/graphene interdigitated gold electrode piezoelectric sensor for rapid and specific detection of Staphylococcus aureus, Biosens. Bioelectron. 65 (2015) 314–319.
[27] N.G. Bastús, J. Comenge, V. Puntes, Kinetically controlled seeded growth synthesis of citrate-stabilized gold nanoparticles of up to 200 nm: size focusing versus Ostwald ripening, Langmuir 27 (2011) 11098–11105.
[28] Z. Cheng, R. Wang, Y. Xing, L. Zhao, J. Choo, F. Yu, SERS-based immunoassay using gold-patterned array chips for rapid and sensitive detection of dual cardiac biomarkers, Analyst 144 (2019) 6533–6540.
[29] H. Yan, Y. You, X. Li, L. Liu, F. Guo, Q. Zhang, D. Liu, Y. Tong, S. Ding, J. Wang, Preparation of RGD peptide/folate acid double-targeted mesoporous silica nanoparticles and its application in human breast cancer MCF-7 cells, Front. Pharmacolo 11 (2020) 898.
[30] B.M. Chen, T.L. Cheng, S.R. Roffler, Polyethylene glycol immunogenicity: theoretical, clinical, and practical aspects of anti-polyethylene glycol antibodies, ACS Nano 15 (2021) 14022–14048.
[31] H. Wang, Z. Song, S. Li, Y. Wu, H. Han, One stone with two birds: functional gold nanostar for targeted combination therapy of drug-resistant Staphylococcus aureus infection, ACS Appl. Mater. Interfaces 11 (2019) 32659–32669.
[32] E.P. Diamandis, T.K. Christopoulos, The biotin-(strept)avidin system: principles and applications in biotechnology, Clin. Chem. 37 (1991) 625–636.